Resolving power of 35,000 (5 mA) in the extreme ultraviolet employing a grazing incidence spectrometer

Michael C. Hettrick, James H. Underwood, Philip J. Batson, and Mark J. Eckart

Applied Optics Vol. 27, Issue 2, pp. 200-202 (1988)

http://dx.doi.org/10.1364/AO.27.000200

RAPID COMMUNICATIONS

This section was established to reduce the lead time for the publication of Letters containing new, significant material in rapidly advancing areas of optics judged compelling in their timeliness. The author of such a Letter should have his manuscript reviewed by an OSA Fellow who has similar technical interests and is not a member of the author's institution. The Letter should then be submitted to the Editor, accompanied by a LETTER OF ENDORSEMENT FROM THE OSA FELLOW (who in effect has served as the referee and whose sponsorship will be indicated in the published Letter), A COMMITMENT FROM THE AUTHOR'S INSTITUTION TO PAY THE PUBLICATIONS CHARGES, and the signed COPYRIGHT TRANSFER AGREEMENT. The Letter will be published without further refereeing. The latest Directory of OSA Members, including Fellows, is published in the July 1987 issue of Optics News.

Resolving power of 35,000 (5 mÅ) in the extreme ultraviolet employing a grazing incidence spectrometer

Michael C. Hettrick, James H. Underwood, Philip J. Batson, and Mark J. Eckart

Michael Hettrick is with Hettrick Scientific, P.O. Box 8046, Berkeley, California 94707; M. J. Eckart is with Lawrence Livermore Laboratory, Livermore, California 94550; the other authors are with Lawrence Berkeley Laboratory, Center for X-Ray Optics, Berkeley, California 94720.

Received 19 October 1987.
Sponsored by J. A. M. Samson, University of Nebraska.
0003-6935/88/020200-03$02.00/0.

We have experimentally verified the performance predicted for a high-resolution spectrometer employing a varied line-space plane reflection grating.[1] Figure 1 illustrates the essential features of the optical system, consisting of a spherical mirror which accepts the incoming divergent light and produces a convergent beam incident to the grating in its plane of dispersion. The spacings between adjacent grooves in the grating surface are determined so as to produce minimum defocusing at a fixed detection position as the grating is rotated about its central groove to scan wavelength. In this geometry, the entrance slit and detector are both fixed in position. This requires the following focusing condition:

$$\frac{r'}{r} = \frac{\cos^2\beta_2(\sin\beta_1 - \sin\alpha_1) - \cos^2\beta_1(\sin\beta_2 - \sin\alpha_2)}{\cos^2\alpha_2(\sin\beta_1 - \sin\alpha_1) - \cos^2\alpha_1(\sin\beta_2 - \sin\alpha_2)}, \quad (1)$$

where r is the distance to the reflected focus of the entrance slit, r' is the image distance, α is the angle of incidence, and β is the angle of diffraction. All distances and angles are relative to the center of the grating. The subscripts denote two wavelengths where the geometrical aberrations of the grating are minimized by a single variation in the groove spacings.

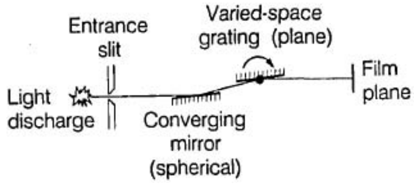

Fig. 1. Optical layout of the high-resolution spectrometer. A plane varied line-space grazing incidence grating is simply rotated (arrow) about its central groove to tune the wavelength band without introducing significant aberration. The focal surface is at normal incidence (i.e., erect) to the diffracted beam.

In the present experiment (Fig. 2) a laboratory Penning light source[2,3] was placed in the proximity of the entrance slit to the spectrograph. The grating was manufactured by the Perkin-Elmer Corp. and had a nominal groove density of 1800 g/mm. The full grating aperture (60 mm) was used for all exposures, yielding a nominal collection angle of 5 mrad in the dispersion plane. A Schumann-type emulsion film (Kodak 101), situated at the focal plane, recorded the astigmatic spectral lines. The exposure time per spectrum was thus quite long, ~2 h. Microdensitometer traces of the film transmission density profiles are shown in Fig. 3 for portions of three spectra centered on selected emission lines. The different wavelength bands were obtained by simply rotating the grating about its central groove. Using a 10-μm slit, the resolving power ($\lambda/\Delta\lambda$) is seen to be ~30,000 at 130 Å and 35,000 at 160 Å. Due mainly to the use of a larger entrance slit width (20 μm), the resolution was reduced to ~16,000 at 208 Å.

An interesting practical result of the narrow singlet Al IV line seen in Fig. 3(b) is that even a coarse monochromator ($\lambda/\Delta\lambda = 100$) can select one or the other of two resonance lines located at 160.073 and 161.686 Å and thus provide a temporally coherent source for interferometry or dispersive microscopy.[4]

The Ne IV doublet seen in Fig. 3(c) represents experimental confirmation of that spectroscopic transition as previously designated[5] to be $2s^22p^3$–$2s^22p^2(^3P)3s^4$. The splitting of this doublet is ~56 mÅ with a similar splitting seen for the other two doublets having the same transition sequence (208.734 and 208.899 Å).

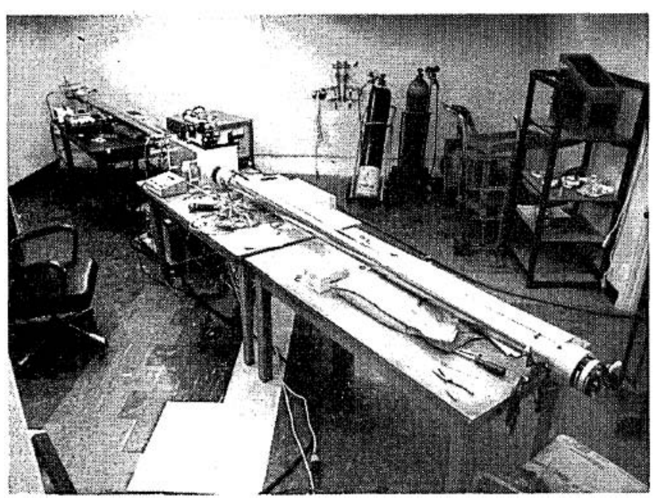

Fig. 2. High-resolution spectrometer, which measures ~6 m in length from the entrance slit to the focal plane. The optics are located in the central chamber located between two 3-m length pipes.

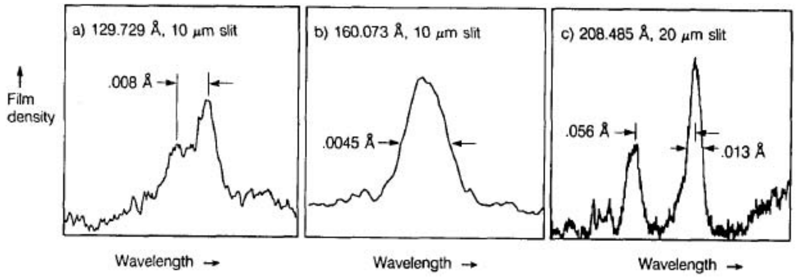

Fig. 3. Microdensitometer trace of film images of a plasma consisting of sputtered aluminum and gaseous neon, where the spectrometer grating is rotated to select different spectral ranges, centered at lines near (a) Al IV 130 Å, (b) Al IV 160 Å, and (c) Ne IV 208 Å. The spectral resolution is seen to be (a) 4, (b) 4.5, and (c) 13 mÅ. A resolution of ~7 mÅ was also obtained for 208 Å when the entrance slit was closed to 10 μm.

The results reported in Fig. 3 were obtained in anticipation of the use of this instrument to measure the linewidths of neonlike species such as selenium and yttrium, which have been shown to exhibit lasing at wavelengths near the regions tested here.[6] In those experiments, throughput will be dramatically increased by use of a premirror to remove astigmatism at the focal plane,[1] and a second pre-mirror will be used to focus the narrow emitting region onto the entrance slit of the spectrometer.

A second consequence of the varied-space grating geometry discussed above, employing a converging beam incident to the grating, is that the focal surface is approximately flat and perpendicular to the principal dispersed ray. The line profiles shown in Fig. 3 were in fact taken over different regions along 25-mm lengths of film, which subtended a spectral range of 1.8–4.0 Å depending on wavelength setting. Unlike the conventional Rowland circle geometry, this normal incidence focal plane geometry facilitates use of high-efficiency detection systems and results in a finite magnification (or demagnification) of the entrance slit. This will be used to advantage when coupled to an electronic detector, as the spectral images were designed to be magnified images of the entrance slit, thus minimizing the effect of large detection pixels. The resulting plate scales for the spectra shown in Fig. 3 are 0.158, 0.125, and 0.071 Å/mm, respectively. Therefore, the resolving power of 30,000 presented in this work is maintained if the detector has a spatial resolution of better than 40 μm. However, even if the detector resolution is 125 μm, the resolving power will be 10,000 on average over the 100–250-Å spectral region.

Our demonstrated resolution exceeds that of previous high-resolution spectrometers or monochromators by a factor of ~10 in this wavelength region.[7–11] The reasons for this large improvement include the ease of alignment due to the normal incidence focal plane, the diffraction-limited optics due to use of only plane and spherical reflective surfaces, and the fixed entrance slit and focal plane.

To exemplify the type of new spectroscopic opportunity made possible by this order of magnitude increase in resolution, the spectrum of autoionized lines of Al III was recorded at a resolution of ~6 mÅ and a section of the microdensitometer trace is shown in Fig. 4. This trace reveals fine structure of the order of 10 mÅ within a line complex located near 171.2 Å. A more complete spectrum of the autoionized Al III sequence revealed twelve spectral lines between ~169.0 and 174.5 Å, consistent with previous theoretical predictions.[2]

In a simpler configuration, the optical system show in Fig. 1 becomes a monochromator by placing an exit slit at the focal plane. The advantage of fixed slits combined with high resolution and the use of only plane and spherical reflective surfaces is self-evident for applications involving immovable and bright sources, such as synchrotron radiation.[12] The physical parameters and phase space acceptance of the present instrument (6 m in length, 10-μm entrance slit, 5-mrad vertical acceptance) are ideally suited for a synchrotron radiation beamline. With the entrance aperture closed to 1.5 mrad, a resolving power of 30,000 will be maintained over a factor of 3 wavelength scan (e.g., 80–250 Å). Due to the grating magnification of the entrance slit, the exit slit width would be larger and depend on the wavelength.

The authors would like to gratefully acknowledge discussions with and support from Dennis Matthews. The authors also thank G. Hirst and S. Coles of the Perkin-Elmer Corp. for diligent efforts in fabrication of the grating, R. Delano for machining of the instrument, and R. Burkard for assistance with the microdensitometry. This work was supported by the U.S. Department of Energy through contracts DE-AC03-76SF00098 and W-7405-ENG-48. The results reported here were obtained when MCH was affiliated with the Center for X-ray Optics of the Lawrence Berkeley Laboratory.

References

1. M. C. Hettrick and J. H. Underwood, "Varied-Space Grazing Incidence Gratings in High Resolution Scanning Spectrometers," AIP Conf. Proc. **147,** 237 (1986).
2. E. S. Warden and H. W. Moos, "Penning Discharge as a Photoelectric EUV Spectroscopy Source," Appl. Opt. **16,** 1902 (1977).
3. D. S. Finley, S. Bowyer, F. Paresce, and R. F. Malina, "Continuous Discharge Penning Source with Emission Lines Between 50 Å and 300 Å," Appl. Opt. **18,** 649 (1979).

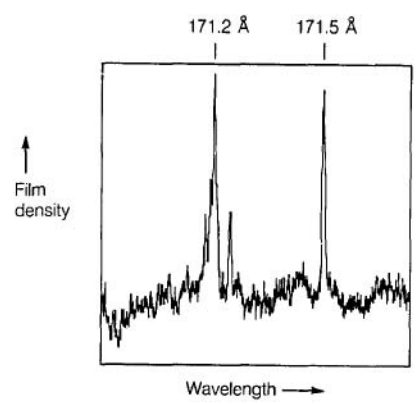

Fig. 4. Microdensitometer trace of film images of sputtered Al III autoionized sequence. The resolving power of 25,000–30,000 results in the separation of several previously undiscovered lines. Approximate wavelengths are indicated.

4. M. C. Hettrick, "Aplanatic Grazing Incidence Diffraction Grating: a New Optical Element," Appl. Opt. **25,** 3269 (1986).
5. F. W. Paul and H. D. Polster, Phys. Rev. **59,** 424 (1941).
6. D. L. Matthews *et al.*, "Demonstration of a Soft X-Ray Amplifier," Phys. Rev. Lett. **54,** 110 (1985).
7. W. R. Hunter, R. T. Williams, J. C. Rife, J. D. Kirkland, and M. N. Kabler, "A Grating/Crystal Monochromator for the Spectral Range 5 eV to 5 keV," Nucl. Instrum. Methods **195,** 141 (1982).
8. H. Peterson, "The High Energy Plane Grating Monochromators at BESSY," Nucl. Instrum. Methods **A246,** 260 (1986).
9. S. L. Hulbert, J. P. Stott, and F. C. Brown, "An Extended Range Soft X-ray Beam Line for the 1-GeV Storage Ring Aladdin," Nucl. Instrum. Methods **208,** 43 (1983).
10. E. Janitti, P. Nicolosi, and G. Tondello, "Stigmatic Observations of Laser-Produced Plasmas with a Grazing-Incidence Spectrograph," Opt. Lett. **4,** 187 (1979).
11. J. L. Schwob, A. W. Wouters, S. Suckewer, and M. Finkenthal, "High-Resolution Duo-Multichannel Soft X-Ray Spectrometer for Tokamak Plasma Diagnostic," submitted to J. Opt. Soc. Am.
12. M. C. Hettrick, "High Resolution Gratings for the Soft X-Ray: Aberration Correction Methods and Their Limitations," in *Proceedings, Synchrotron Radiation Instrumentation Conference* (Madison, WI, 1987), to appear in Nucl. Instrum. Methods (1988).

Folded perfect shuffle optical processor

Charles W. Stirk, Ravindra A. Athale, and Michael W. Haney

BDM Corporation, 7915 Jones Branch Drive, McLean, Virginia 22102.
Received 25 September 1987.
Sponsored by J. W. Goodman, Stanford University.
0003-6935/88/020202-02$02.00/0.

The perfect shuffle interconnection network (PS) consists of splitting a linear array of $N = 2^n$ items in half and interleaving the two halves. The PS was originally proposed as the interconnection primitive between local processors for parallel computation of the fast Fourier transform polynomial evaluation, sorting, and matrix transposition.[1] Interconnection permutations necessary for parallel matrix computations other than matrix transpose also were realized on the PS.[2] For the more general routing problems found in MIMD machines and telecommunications networks, an algorithm was presented to connect an arbitrary permutation of inputs to outputs with a limited number of PS stages [$O(\log N)$].[3] A review of the parallel computation abilities of the PS is conducted in Ref. 4.

The wide utility of PS networks led to attempts to map the PS onto VLSI architectures.[5,6] The inherent VLSI wiring characteristics of capacitive and inductive crosstalk, length-dependent power requirements, timing skew, limited crossovers, and chip area are ill-suited to the global and space-variant nature of the PS. Thus a trade-off of local processing complexity, the number of parallel channels and signal bandwidth due to the practical limitations of VLSI, limits the applicability of electronic PS implementations.

The ability of light beams to carry high-bandwidth data through free space without mutual coupling, the independence of drive power and interconnection length, the minimal timing skew, and the 3-D nature of optical systems led to suggestions of optical interconnects for electronic processors.[7] The space–bandwidth product of optical systems (10^6) limits the number of parallel channels, while the modulation speed (10 GHz) and degree of multiplexing (wavelength and polarization) limit the channel bandwidth. By using optical communications the overall system throughput is increased by eliminating the interconnection network bottleneck. Hence free-space optics appears ideal for implementation of the PS in applications with high data rates or many parallel channels like telecommunications and fine-grained parallel processors.

The earliest proposed free-space optical architectures for the PS[8,9] are capable of shuffling either the rows or columns of a matrix. If each data word is recorded as a column, shuffling between the columns results in a bit-parallel PS. In such spatially multiplexed architectures the maximum length of the data words must be known *a priori*. With time-multiplexed data streams, however, the word length is unlimited, and the other spatial dimension is free to encode additional data channels. Moreover, in many cases, the subsystems connected by the PS provide and require serial data. A 2-D optical PS was proposed[10] and demonstrated[11] that rearranges a 2-D image of serial data streams by shuffling the rows and columns. The architecture divides and interlaces the matrix along each direction as separate operations. Since the 1- and 2-D PS are different interconnection primitives, not all the routing algorithms and hardware developed for the 1-D PS are compatible with the 2-D PS.

In this Communication we describe an algorithm that performs a 1-D PS on a long 1-D sequence that is raster-formatted on a matrix. We propose optical architectures and hardware to implement the algorithm and show experimental results for a particular system. The proposed algorithm and architectures retain compatibility with the well-developed 1-D PS algorithms while taking full advantage of the 3-D interconnection capabilities and 2-D space–bandwidth of free-space optics. Because a similar philosophy was employed in designing 2-D optical systems to perform spectrum analysis of very long (10^6) raster-recorded 1-D time signals in the work on the folded spectrum analyzer,[12,13] we call our processor the folded perfect shuffle optical processor.

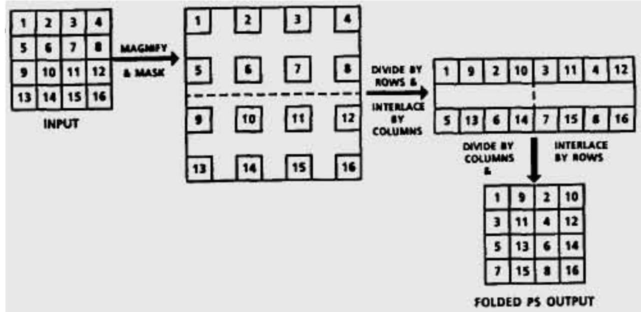

Fig. 1. Two-step approach to the folded PS.

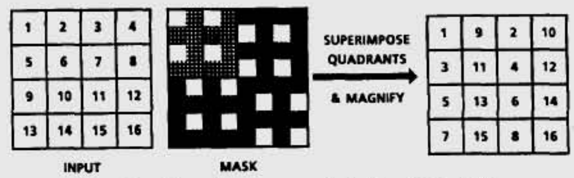

Fig. 2. One-step approach to the folded PS.